Neural network approach to 5G digital modulation recognition under a priory uncertainty of parameters

Bohdan Kotyk[1,†], Denys Bakhtiiarov[1,2,†], Bohdan Chumachenko[1,*,†], Yuliia Burmak[1,†], Serhii Chumachenko[1,†] and Oleksandr Lavrynenko[1,†]

[1]State University "Kyiv Aviation Institute", Liubomyra Huzara Ave., 1, Kyiv, 03058, Ukraine
[2]State Scientific and Research Institute of Cybersecurity Technologies and Information Protection, Maksym Zalizniak Str., 3/6, Kyiv, 03142, Ukraine

Abstract

In digital communication, the correct identification of modulation types has huge importance, and it can enhance the reliability of signal processing. This work describes an approach to recognizing digital modulation types when the signal parameter, carrier frequency, initial phase, etc., is uncertain. The basis of the classification method is the 9th order of cumulants— indeed, it is the key feature enabling an accurate classification. This article employs a multilayer neural network, which, in turn, is combined with a data normalization scheme to determine possible modulation type factors (i.e., QAM–8, APSK–8, QAM–64, PSK–8) even when the corresponding parameter factors are unknown. The results of the simulation study indicate that suboptimal performance of the system has almost been eliminated concerning present inaccuracies in carrier frequency offset or initial phase offset. Thus, this methodology can easily be used as a firm base extending to other modulation types and, thus, to similar uncertainties in other signal parameters.

Keywords

machine learning, neural network, 5G, high order cumulants, digital modulation, ReLU, softmax, backpropagation

1. Introduction

In a previous paper, we formulated and solved the problem of the recognition of digital modulation in 5G systems under the assumption of perfectly synchronous receivers. That study had been motivated by the need for ultra-precise classification of signals in the context of advanced communication and had proposed a neural-network-based approach that secures fairly good identification of very weak signals—if accompanied by statistical features of the signals—at low SNR values [1, 2]. Statistical features that were chosen are high-order mixed cumulants $C_{n,m}$, which could be described in formulas of their relation to mixed moments $E_{n,m}$ up to the 9-th order from $C_{2,0}$:

$$C_{2,0} = E_{2,0}, \tag{1}$$

to $C_{5,4}$:

$$\begin{aligned} C_{5,4} = {} & E_{5,4} - 10E_{4,4}E_{2,0} - 20E_{4,3}E_{1,1} - 6E_{5,2}E_{0,2} - 10E_{4,2}E_{3,0} - 40E_{3,3}E_{2,1} - 30E_{4,2}E_{1,2} \\ & -3E_{5,1}E_{0,3} - E_{5,1}E_{0,2} - 5E_{1,4}E_{4,0} - 40E_{3,2}E_{3,1} - 60E_{4,1}E_{2,2} - 20E_{4,1}E_{1,3} - E_{5,0}E_{0,4} + \\ & 30E_{1,4}E^2 + 60E_{2,3}E_{1,1}E_{2,0} + 180E_{4,2}E_{0,2}E_{2,0} + 240E_{4,1}E_{3,1}E_{2,0} + 120E_{3,2}E_{2,0}E_{1,1} + \\ & 111E_{4,1}E_{1,0}E_{0,2} + 4E_{5,0}E_{0,2} + 10E_{4,1}E_{1,1} + 2E_{5,0}E_{0,2} + 300E_{2,2}E_{1,2}E_{2,0} + 60E_{2,2}E_{1,1}E_{2,0} + \end{aligned} \tag{2}$$

CH&CMiGIN'25: Fourth International Conference on Cyber Hygiene & Conflict Management in Global Information Networks, June 20–22, 2025, Kyiv, Ukraine

*Corresponding author.
†These authors contributed equally.
3351920@stud.nau.edu.ua (B. Kotyk); bakhtiiaroff@tks.kai.edu.ua (D. Bakhtiiarov); bohdan.chumachenko@npp.kai.edu.ua (B. Chumachenko); yu.burmac@ukr.net (Y. Burmak); serhii.chumachenko@npp.kai.edu.ua (S. Chumachenko); oleksandrlavrynenko@tks.kai.edu.ua (O. Lavrynenko)
0009-0005-0821-9108 (B. Kotyk); 0000-0003-3298-4641 (D. Bakhtiiarov); 0000-0002-0354-2206 (B. Chumachenko); 0000-0002-5410-6260 (Y. Burmak); 0009-0003-8755-5286 (S. Chumachenko); 0000-0002-3285-7565 (O. Lavrynenko)

$$270E^2E_{1,2}E_{2,0} + 720E_{1,1}E_{1,2}E_{2,0} - 360E_{1,2}E_{2,0}E_{0,2} - 720E_{1,1}E_{1,2}.$$

The architecture and implementation of an MLP were specifically optimized for modulation recognition is described. The network takes signal features through an input layer, nonlinearly transforms the inputs via multiple hidden layers with ReLU activations and makes a probability-based classification through a Softmax output layer. That is, the processing stages, which is in weighted sums and application of nonlinear transformations as discussed in:

$$df_j = \text{act}^{(j,1)} = w_0^{(j,1)} + \sum_{i=1}^{n} w_i^{(j,1)} x_i \tag{3}$$

where $w^{(j,1)} = \left(w_0^{(j,1)}, w_1^{(j,1)}, w_n^{(j,1)}\right), j = (1, N_1)$ - row vector of synaptic connections for the j-th neuron N_1 - Number of neurons in the input layer, n - Number of input features, x_i - Row vector of the i-th input.

And the subsequent related formulas which govern the activations of the neurons, and also the backpropagation weight updates are presented. The principal novelty of this research emanates from the aviation of high-order cumulants as good descriptors to take into consideration the inherent statistical properties of modulated signals. Some of the properties of cumulants that have been revealed include their resistance to the characteristic Gaussian noise and ability to resolve distinctions between various modulation schemes. This difference summarized the moments and that was a positive groundwork toward distinguishing the different modulations, for example, QAM and PSK, among several others [3, 4, 5].

That dataset comprised 10,000 signal samples for training and was later broken down into training, validation, and testing datasets. The optimization of the neural network used the Adam algorithm. Another model that reported having an SNR of 5 dB and three hidden layers configured to give just about 99% recognition accuracy was reported [6, 7]. That subsection also elaborates on how changes in the architecture of the network and the hidden layer number influence performance; this injects more evidence towards the effective performance of cumulant-based feature extraction and neural training process.

A multilayer perceptron optimized with Adam using high-order cumulants for feature descriptors presents itself as a dependable methodology for recognition of digital modulations under ideal synchrony.

In modern information transmission systems, the transmitted signal may contain service information for synchronization between the transmitter and receiver, but often upon reception of the signal its carrier frequency and initial phase are known with some error. For example, this occurs when analyzing the received signal in the case of the Doppler effect, when the frequency of the received oscillations changes according to a law associated with the movement of the transmitter and receiver of these oscillations, or, for example, due to the instability of the frequencies of the transmitter and the heterodynes of the receiver [8, 9, 10].

In this article, we study the problem of recognizing the types of digital modulation of the received signal with parametric a priori uncertainty, in particular, uncertainty of the carrier frequency or initial phase. The received high-frequency signal is subjected to preliminary processing, where the received signal is transferred to the zero frequency by multiplying by the oscillations $\cos(2\pi f_0 t + \phi_0)$, and $\sin(2\pi f_0 t + \phi_0)$, generated by the heterodyne, the received signal is passed through a low-pass filter and discretized for further digital processing. As a result of preliminary processing, the received signal can be expressed as follows:

$$r_k(t) = \frac{1}{2} A(t) \left\{ \cos\left[2\pi \Delta f t + \theta(t) + \Delta\theta_0\right] - i \sin\left[2\pi \Delta f t + \theta(t) + \Delta\theta_0\right] \right\} = I_k(t) + iQ_k(t), \tag{4}$$

where Δf is the carrier frequency offset, and $\Delta\theta_0$ is the initial phase offset.

The obtained in-phase $I_k(t)$ and quadrature $iQ_k(t)$ components are grouped into a complex signal $r_k(t) = I_k(t) + iQ_k(t)$ and its complex conjugate $r_k^*(t) = I_k(t) - iQ_k(t)$, which are the initial data for calculating the moments and cumulants. To overcome a priori uncertainty, it is proposed to continue

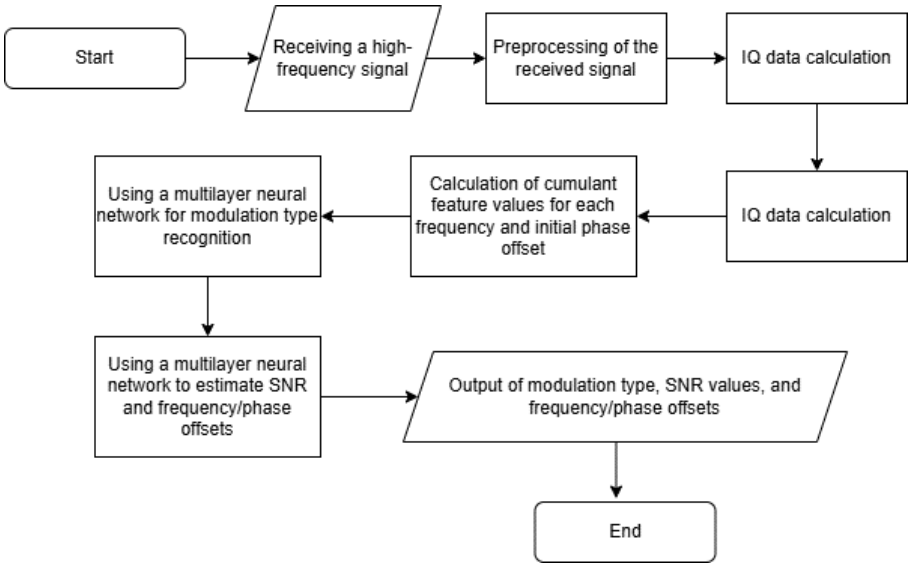

Figure 1: Algorithm for recognizing types of digital signal modulation with parametric a priori uncertainty.

using the capabilities of a neural network. This requires an increase in the number of hypotheses tested by the neural network. For example, with completely known signal parameters, there was only one hypothesis that the signal had PSK-8 modulation. With the unknown signal frequency, the hypotheses have appeared that the signal modulation is PSK-8, and the frequency shift is 0 Hz; that the signal modulation is PSK-8 and the frequency shift is 500 Hz; and so on. Figure 1 shows an algorithm for recognizing modulation types and estimating the value of the detuning from the carrier frequency or the initial phase using high-order cumulants as informative features [11, 12, 13].

Table 1
Values of Cumulants of Different Orders for QAM-64 and PSK-8 Modulation

Cumulant	**QAM-64**		**PSK-8**	
	$\Delta f = 0$ and $\Delta\theta_0 = 0$	$\Delta f = 900$ Hz	$\Delta\theta_0 = 0.04$ rad.	$\Delta f = 900$ Hz
$C_{2,0}$	-0.00914	-0.00631	0.012098	-0.01226
$C_{3,0}$	-0.03608	0.047022	-0.04646	0.040557
$C_{2,1}$	-0.00801	0.004393	0.013821	0.013631
$C_{4,0}$	-0.56475	-0.01767	3.126333	3.203364
$C_{4,2}$	-0.61434	-0.98048	0.920861	0.85352
$C_{5,0}$	-0.20752	0.092887	0.044091	0.058086
$C_{3,2}$	-0.00931	-0.00627	-0.05668	0.013849
$C_{6,0}$	0.050119	-0.06521	0.977919	1.334189
$C_{3,3}$	1.629901	3.845417	-0.99971	-0.56647
$C_{7,0}$	-1.56306	-0.4735	-1.01194	0.513651
$C_{6,1}$	0.599746	-0.50621	-1.2013	-1.02816
$C_{4,3}$	-0.12934	0.010309	-0.3314	-0.7638
$C_{8,0}$	-12.8893	-1.42314	-192.062	-202.193
$C_{6,2}$	-11.6764	0.01108	-28.292	-22.645
$C_{4,4}$	1357.575	1414.858	1412.948	1360.68
$C_{9,0}$	-8.1217	4.105405	-28.8553	-15.8736
$C_{8,1}$	6.432584	5.206349	27.08937	-7.69605
$C_{6,3}$	-121.758	114.9256	535.0172	368.783
$C_{5,4}$	2470.2	2219.866	5224.992	4881.125

In contrast to the algorithm studied in previous work, in this case the cumulants for different types of modulation are calculated at a specific SNR value, and the offset from the carrier frequency varies from 0 Hz to 2000 Hz with a step of 500 Hz, and the offset from the initial phase - from 0 rad. to 0.09

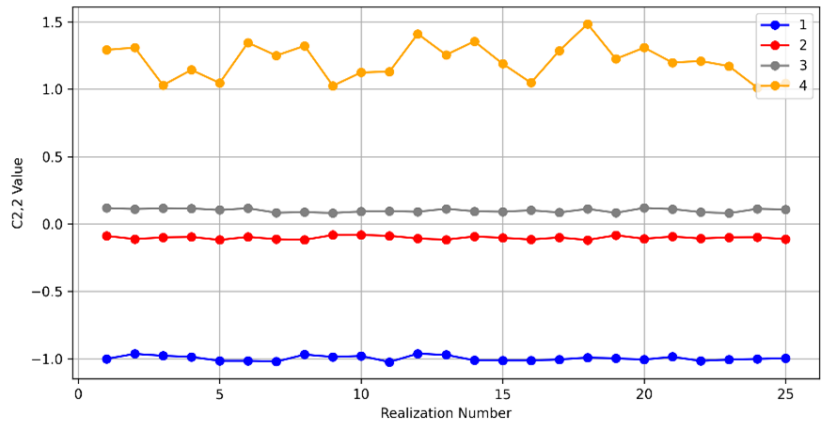

Figure 2: Graph of the distribution of the $C_{5,4}$ value for GMSK at different values of Δf.

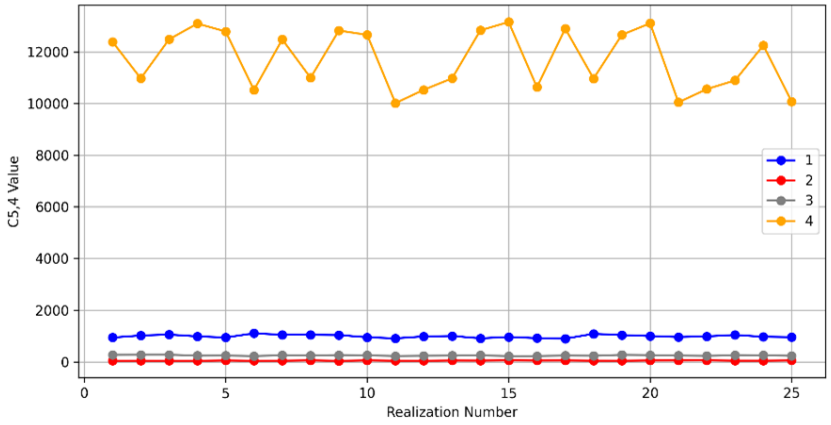

Figure 3: Distribution graph of the $C_{5,4}$ value for GMSK at different values of Δf.

rad. with a step of 0.01 rad. Despite the fact that in this case it is necessary to have a large number of databases for the ANN input, this method does not require an additional algorithm for estimating the value of the carrier frequency and the initial phase [14, 15]. This algorithm is uniform and allows recognizing the types of digital modulation of the received signal with an acceptable time spent in the process of processing the received signal. Table 1 shows examples of cumulant values up to the 9th order for QAM-64 and PSK-8 modulation with different values of the carrier frequency offset Δf and the initial phase $\Delta\theta_0$ at SNR = 3 dB. The analysis of the obtained cumulant values allows us to assert that the information content of one or another cumulant about the type of signal modulation depends significantly on the offsets Δf and $\Delta\theta_0$. For example, in the absence of offsets, the first cumulant $C_{2,2}$ in the table for both distinguished types of modulation QAM-64 and PSK-8 has the same negative sign, at $\Delta f = 900$ Hz the signs of the cumulants are different, at $\Delta\theta_0 = 0.04$ rad the signs of the cumulants are positive [16, 17, 18].

Figures 2 and 3 show the dependencies of the cumulant values $C_{2,2}$ and $C_{5,4}$ for the GMSK signal with different values of Δf. At $\Delta f = 0$ Hz (curve 1), $\Delta f = 500$ Hz (curve 2) and $\Delta f = 1000$ Hz (curve 3), the values of the cumulants $C_{2,2}$ and $C_{5,4}$ remain virtually unchanged for different signal realizations, although the values depend on the frequency shift. In the case of $\Delta f = 1500$ Hz (curve 4), the values of the cumulants $C_{2,2}$ and $C_{5,4}$ begin to change noticeably for different realizations.

Figure 4 shows the values of the cumulant $C_{5,3}$ for the GMSK signal at different values of Δf.

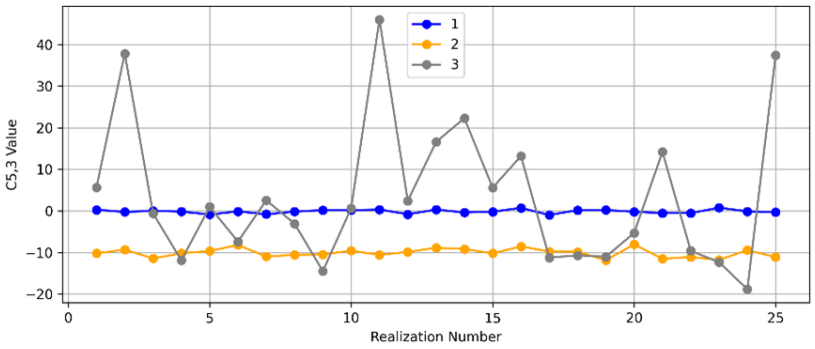

Figure 4: Distribution graph of the $C_{5,3}$ value for GMSK at different values of $\Delta\varphi_0$.

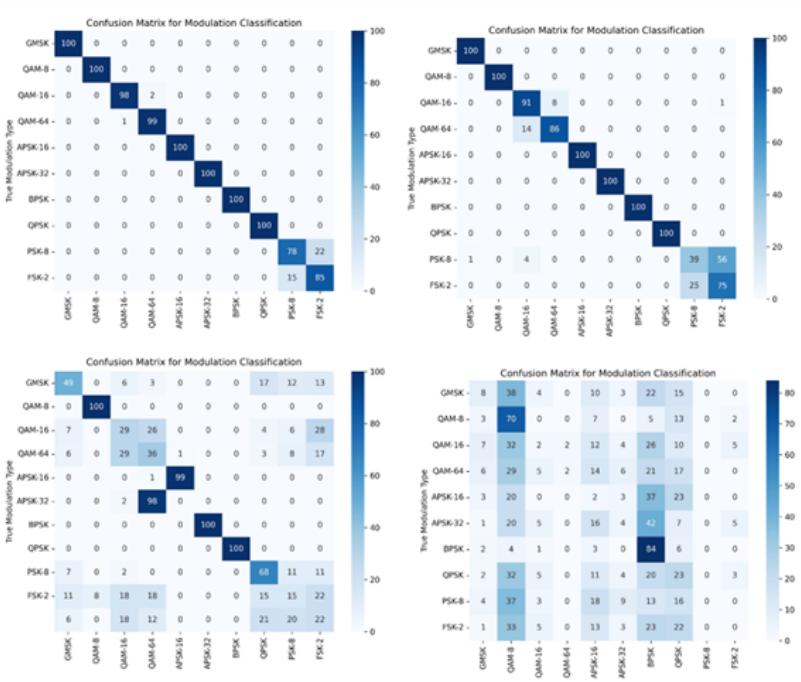

Figure 5: The result of assessing the accuracy of signal modulation recognition at $\Delta\theta_0$ equals 0, 0.02, 0.05, and 0.09 rad.

From the graphs, it is evident that at $\Delta f = 0$ rad. (curve 1) and $\Delta f = 0.02$ rad. (curve 2) the value of $C_{5,3}$ changes insignificantly for different implementations, but the value of cumulants itself depends significantly on the phase shift. And at $\Delta\theta_0 = 0.05$ rad. (curve 3) the value of the cumulant begins to change significantly for different implementations. From the results of cumulant behavior analysis, it may be said that the approximated to cumulant features improve the recognition accuracy of the types of digital modulation of signals for nonzero offsets from the carrier frequency and initial phase [19, 20, 21]. Modeling of a multilayer neural network was done in the Python program. At an SNR of 5 dB, four databases were created for the recognition of types of digital modulation with a priori uncertainty of initial phase. Each database includes 10,000 signals (1000 signals per modulation type), where 7200 signals are for training, 1800 for validation, and 1000 for testing.

Figures 5 show the results of the experimental evaluation of the average value of the accuracy of recognizing types of digital modulation of signals for different values of $\Delta\theta_0$.

It follows from the graphs that at SNR = 5 dB and a value of $\Delta\theta_0 = 0.02$ rad. the average accuracy is 0.891, at $\Delta\theta_0 = 0.05$ rad. for QAM-8, APSK-16, APSK-32 and BPSK modulation the accuracy is 0.99, and for GMSK, QAM-16, QAM-64, QPSK, 8-PSK-8 and FSK-2 modulation the accuracy drops due to the fact

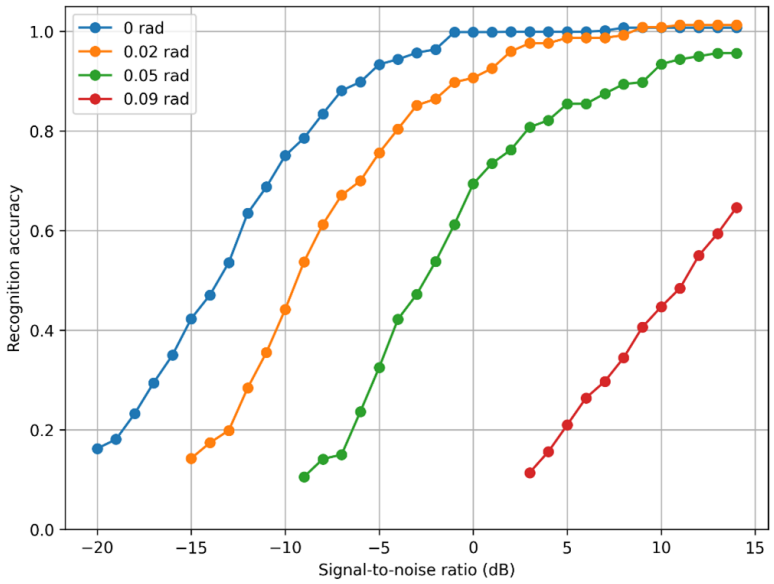

Figure 6: Dependence of recognition accuracy from SNR for different values of $\Delta\theta_0$.

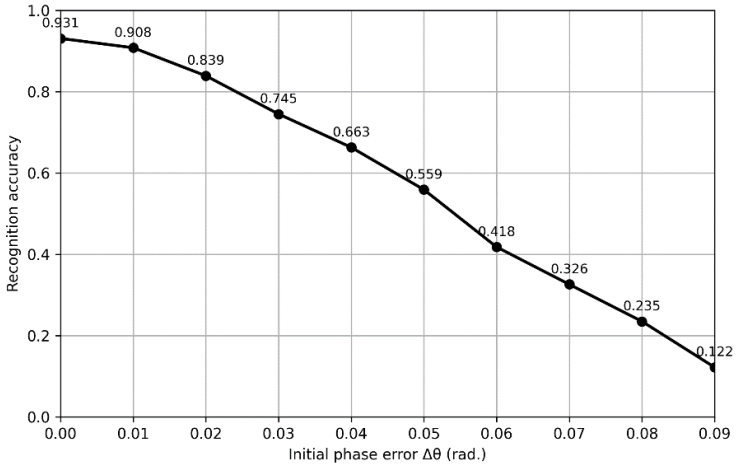

Figure 7: Dependence of recognition accuracy from $\Delta\theta_0$ at SNR = 3 dB.

that the cumulant values have unstable behavior for different signal implementations, and the cumulant values themselves for these types of modulation differ insignificantly [22, 23, 24]. Even at $\Delta\theta_0 = 0.09$ rad., recognition of digital modulation types is practically impossible; the average accuracy is 0.112. To study the influence of the SNR value on the accuracy of recognition of digital modulation types at different values of offset from the initial phase, 71 databases were formed. Each database corresponds to one SNR value, which varies from -20 dB to 14 dB with a step of 0.5 dB. The simulation result is shown in Figures 6 and 7. It is evident from the graphs that with an increase in the offset from the initial phase, the average accuracy of recognition of digital modulation types decreases because high-order cumulants at a large offset from the initial phase have large values [25], which is evident in Figures 2–4.

Similarly, with a priori uncertainty of the carrier frequency, four databases were formed. Figure 8 shows the results of the experimental evaluation of the average value of the accuracy of recognizing types of digital signal modulation for different values of Δf at SNR = 5 dB.

The graphs clearly show that at $\Delta f = 500$ Hz and $\Delta f = 1000$ Hz, the average accuracy for GMSK,

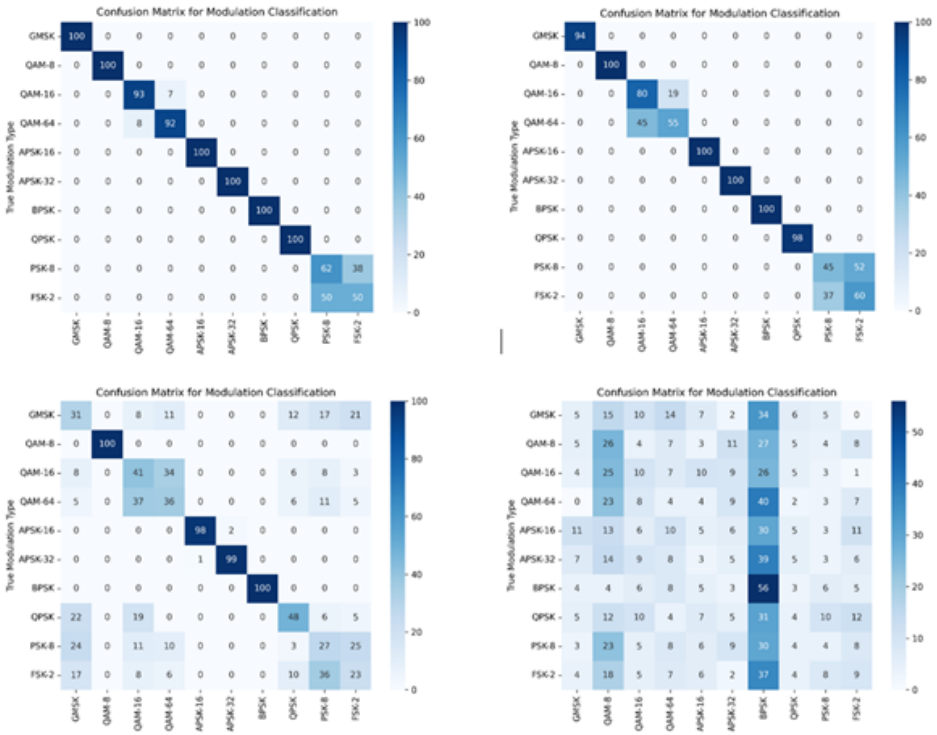

Figure 8: Result of assessing the accuracy of signal modulation recognition at Δf equals 500, 1000, 1500, and 2000 Hz.

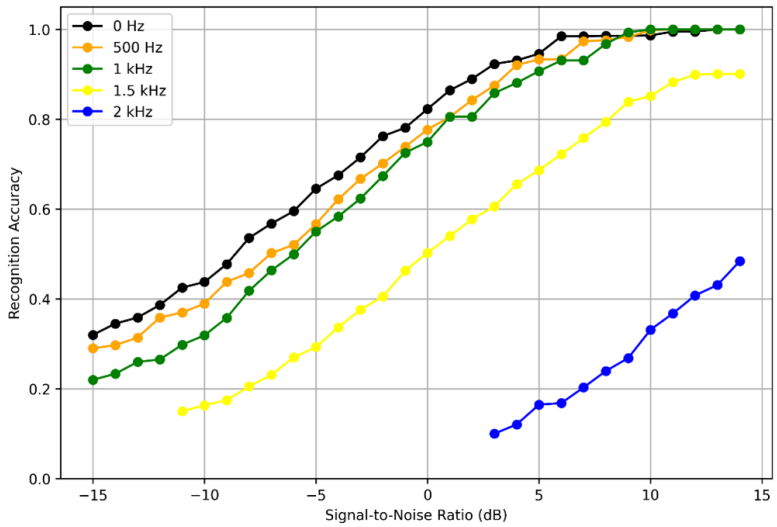

Figure 9: Dependence of recognition accuracy from SNR for different values of Δf.

8-QAM, APSK-16, APSK-32, BPSK and QPSK modulation is greater than 0.94, and for other types of modulation it is significantly lower. At large frequency offsets, for example, at $\Delta f = 1500$ Hz and $\Delta f = 2000$ Hz, the average accuracy is low. 71 databases were created to study the effect of the SNR value on the accuracy of recognizing digital modulation types at different offsets from the carrier frequency. Each database corresponds to one SNR value, which varies from -20 dB to 14 dB with a step of 0.5 dB. The simulation result is shown in Figure 9.

From graphs 6 and 9, we can conclude that in order to ensure acceptable reliability of modulation type recognition by the neural network, the maximum value of Δf should not exceed 1.5 kHz, and the phase shift $\Delta\theta_0$ should not be greater than 0.05 rad.

2. Multilayer perceptron in the problem of recognizing QAM and PSK modulation under parametric a priori uncertainty

The study of the algorithms for recognizing modulation types showed that, compared to the recognition of other modulation types, the separation of QAM-8 and APSK-16, as well as QAM-64 and PSK-8 at low SNRs occurs with less reliability. In this section, a study is conducted on the recognition of these modulation types with uncertainty in the carrier frequency and initial phase [26, 27, 28]. From the graphs of the previous section, it is clear that with large offsets from the carrier frequency or initial phase, the average accuracy of correct recognition of these modulation types decreases due to the fact that high-order cumulants under this condition have a large value compared to low-order cumulants, therefore, the efficiency of the cumulant separation property decreases [29, 30]. For example, in Table 1 at $\Delta f = 900$ Hz for the QAM-64 signal, the value of the cumulant $C_{5,4}$ is greater than the cumulant $C_{2,2}$ in $\frac{5225.74}{0.921} \approx 5680$ times.

It is resolved by applying the Database Standardization process available in the ANN. The standardization method (Standard Scaler) in ML is one of the data preprocessing methods used to scale all original values in the dataset based on values drawn from a distribution with a mean of zero and standard deviation of one. The two steps are appending columns and fitting the model. In the first step, the mean and standard deviation of each feature in the data set are calculated. In the second step, each feature value is transformed according to the formula:

$$Z = \frac{x - \mu}{\sigma}, \tag{5}$$

where x is the original feature value, μ and σ are the mean and standard deviation of the feature.

The standardization method results in a standardized scale that determines the place of each value in the data set by measuring its deviation from the mean in standard deviation units. This makes the data comparable and usable for machine learning. As an example, the cumulant values obtained as a result of standardization for QAM-64 and PSK-8 modulation and certain frequency and initial phase detuning of the signal are presented in Table 2.

Table 2
Cumulant Values Obtained as a Standardization Result

Cumulant	**QAM-64**		**PSK-8**	
	$\Delta f = 0$ and $\Delta\theta_0 = 0$	$\Delta f = 900$ Hz	$\Delta\theta_0 = 0.04$ rad.	$\Delta f = 900$ Hz
$C_{2,0}$	-0,04023	-0,03522	0,092938	-0,07588
$C_{3,0}$	0,001786	-0,04106	-0,03308	0,03591
$C_{2,1}$	0,023648	0,009617	0,017193	0,01704
$C_{4,0}$	-0,43625	-0,43415	-0,42418	-0,42408
$C_{4,2}$	-0,4352	-0,43881	-0,42107	-0,42168
$C_{5,0}$	-0,00614	-0,00639	-0,00661	-0,00656
$C_{3,2}$	-0,00893	-0,00817	-0,00862	-0,00799
$C_{6,0}$	-0,00173	-0,00179	-0,00152	-0,00143
$C_{3,3}$	0,035202	0,036431	0,033832	0,034062
$C_{7,0}$	-0,00902	-0,00903	-0,00904	-0,00901
$C_{6,1}$	-0,01063	-0,01064	-0,01066	-0,01066
$C_{4,3}$	-0,00694	-0,00697	-0,00699	-0,00701
$C_{8,0}$	0,375218	0,375228	0,375183	0,375079
$C_{6,2}$	0,322667	0,322727	0,322649	0,322549
$C_{4,4}$	-0,38261	-0,38257	-0,3825	-0,38248
$C_{9,0}$	-0,00205	-0,00205	-0,00205	-0,00205
$C_{8,1}$	-0,0083	5.-0,0083	-0,00829	-0,0083
$C_{6,3}$	-0,02269	-0,02227	-0,02227	-0,02228
$C_{5,4}$	-0,37805	-0,37809	-0,37811	-0,3781

As a result of standardization of the database for the QAM-64 signal, the ratio between the cumulants $C_{5,4}$ and $C_{2,2}$ decreases to $-0.3782/-0.4208 \approx 0.9$.

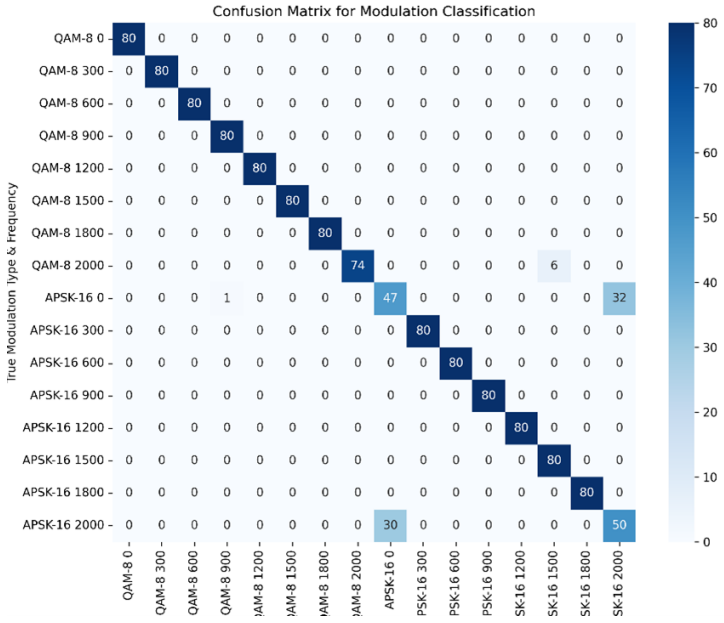

Figure 10: Results of QAM-8 and APSK-16 modulation recognition for different values of Δf.

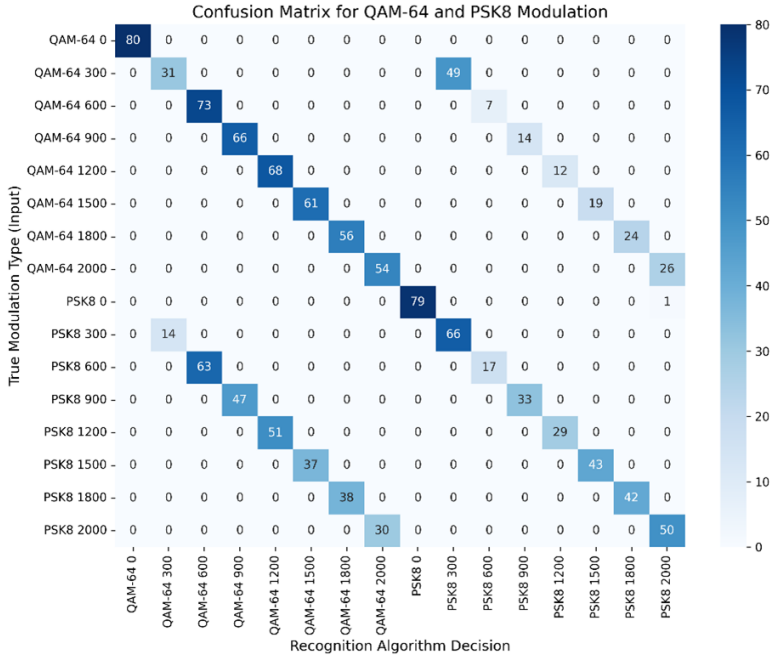

Figure 11: Results of recognition of QAM-64 and PSK-8 modulation for different values of Δf.

Four databases have been formed to recognize two modulation groups: QAM-8 and APSK-16, QAM-64 and PSK-8. The first two databases have been formed to recognize these modulation types under carrier frequency offset conditions; each database consists of 12,800 signals (800 signals for each carrier frequency offset value). Under initial phase offset conditions, two databases have also been formed; each database consists of 16,000 signals (800 signals for each initial phase offset value). The results of modeling the recognition of the modulation type under carrier frequency offset conditions are shown in Figure 10 and 11.

The figures are in the form of tables, the rows and columns of which correspond to the signal

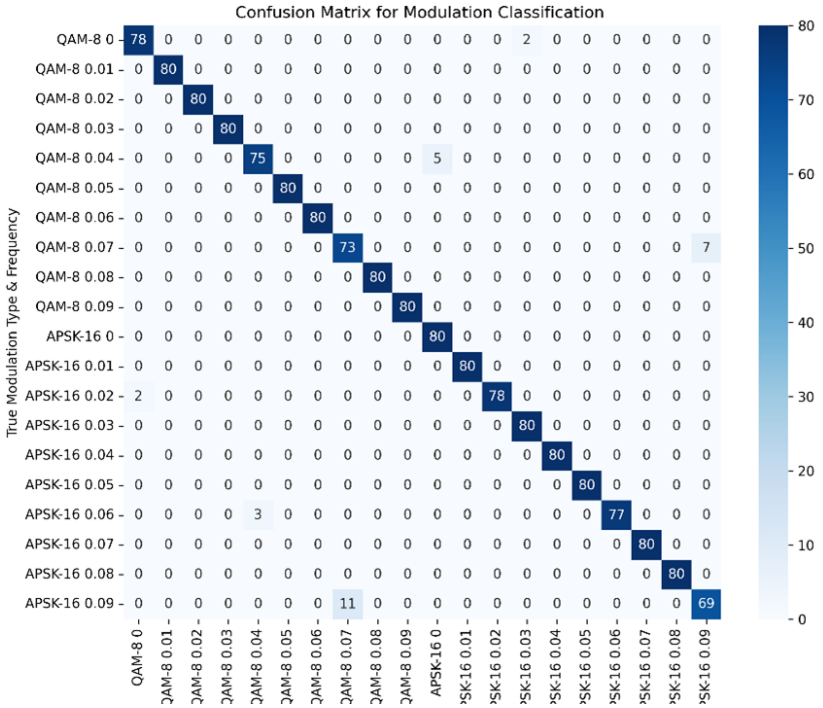

Figure 12: Results of QAM-8 and APSK-16 modulation recognition for different values of $\Delta\theta_0$.

modulation type and carrier frequency offset. The cells contain the results of recognizing the modulation type. For example, for Figure 10: when recognizing QAM-8 signals with a zero-frequency shift (the first row in the figure is QAM-8 0), all 80 signals involved in the computer experiment were recognized correctly. When recognizing a QAM-8 signal with a frequency shift of 1800 Hz (QAM-8 1800), 75 signals were recognized correctly, and an erroneous decision was made for five signals that it was APSK-16 1800. The figures clearly show that the use of a multilayer neural network allows not only recognizing modulation types, but also determining the carrier frequency offset values [31, 32]. Above, the accuracy of recognizing a certain modulation type was understood as the probability of correctly identifying this type of signal modulation among all the modulation types under consideration. In the modeling, this probability was estimated as a sample average, i.e., as the ratio of the number of correctly recognized signals with a given modulation type to the total number of realizations of different signals involved in the computer experiment [33, 34, 35]. Recognition accuracy is of QAM-8 and APSK-16 modulations with different values, thus, 0.96. Figure 12 and Figure 13 show recognition results when an Initial Phase Offset condition was used.

It can be seen from Figures 11 and 13 that the accuracy of QAM-64 and PSK-8 modulation recognition decreases at large frequency and phase detuning. Values of multiple cumulants at large detuning show unstable behavior when it comes to different implementations of signals, whereas the values of these multiple cumulants for particular modulation types vary insignificantly. However, the use of a multilayer neural network ensures high accuracy in estimating the values of Δf and $\Delta\phi_0$.

Figure 14 shows the results of an experiment on recognizing a received signal with an unknown value of Δf. The experiment showed that the accuracy of recognition is 0.53 for QAM-64 modulation and 0.47 for PSK-8 modulation. At the same time, the value of detuning from the carrier frequency Δf, equal to 600 Hz, is determined by the algorithm with high reliability.

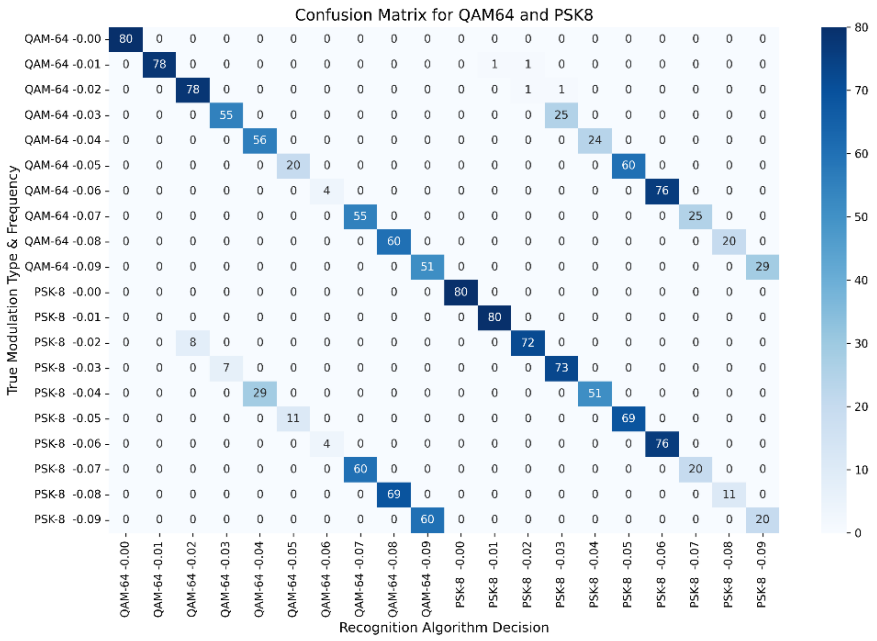

Figure 13: Results of QAM-64 and PSK-8 modulation recognition for different values of $\Delta\theta_0$.

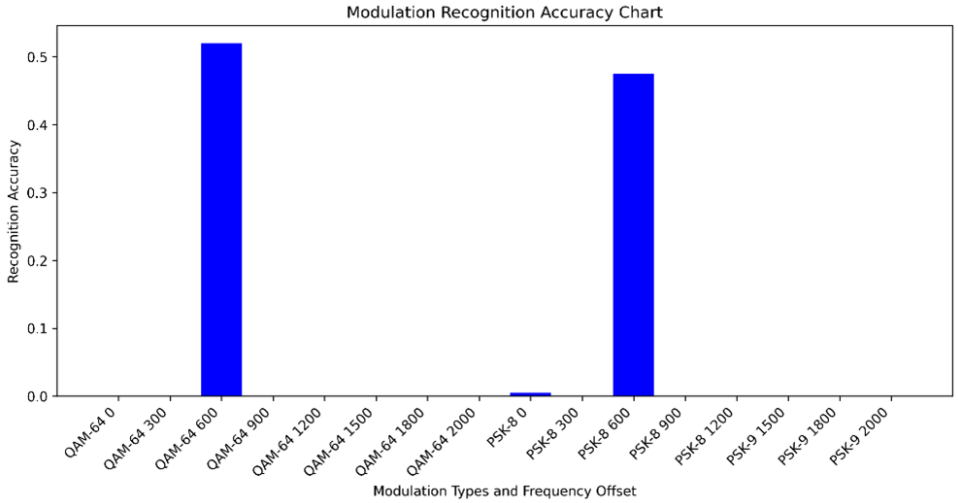

Figure 14: Modulation Recognition Accuracy for Different QAM-64 and PSK-8 Modulation Types with Varying Frequency Offsets.

3. Conclusions

This article considers the approach to recognize digital modulation types of signals in cases of inaccurate knowledge of signal parameters, including the carrier frequency and initial phase. It shows that to recognize signal modulation types, it is preferable to use cumulants up to the 9th order. The simulation results have confirmed that in the region of small values of either the carrier frequency offset or the initial phase of the signal, this method indeed ensures high accuracy in recognizing modulation types. Furthermore, the results of the simulation give us the possibility and advisability of expanding the list of classified modulation types. A method of recognizing digital modulation types (QAM–8, APSK–8, QAM–64, PSK–8), in the case of inaccurate knowledge of signal parameters, including the carrier frequency and initial phase, is considered. A multilayer neural network is built. Data normalization is used as a data preparation technique. Simulation results confirm that in the case of inaccurate determination of carrier frequency and initial phase, a multilayer neural network using cumulants as an

information feature can not only recognize types of digital modulation with high probability but also estimate the very values. The technique applied to solving the problem of a priori uncertainty about the parameters of the signal can be applied to the case of simultaneous uncertainty about values of the carrier frequency and initial phase, as well as the amplitude of the signal, its time position, etc.

Declaration on Generative AI

The authors have not employed any Generative AI tools.

References

[1] D. I. Bakhtiiarov, G. F. Konakhovych, O. Y. Lavrynenko, An approach to modernization of the hat and cost 231 model for improvement of electromagnetic compatibility in premises for navigation and motion control equipment, in: 2018 IEEE 5th International Conference on Methods and Systems of Navigation and Motion Control (MSNMC), 2018, pp. 271–274. doi:10.1109/MSNMC.2018.8576260.

[2] B. Kotyk, D. Bakhtiiarov, O. Lavrynenko, B. Chumachenko, V. Antonov, V. Fesenko, V. Chupryn, Neural network approach to 5g digital modulation recognition, in: Proceedings of the Workshop on Cyber Hygiene Conflict Management in Global Information Networks, volume 3925 of *CEUR Workshop Proceedings*, 2025, pp. 82–92. URL: https://ceur-ws.org/Vol-3925/paper07.pdf.

[3] D. Bakhtiiarov, O. Lavrynenko, N. Lishchynovska, I. Basiuk, T. Prykhodko, Methods for assessment and forecasting of electromagnetic radiation levels in urban environments, Informatyka, Automatyka, Pomiary w Gospodarce i Ochronie Środowiska 11 (2021) 24–27. doi:10.35784/iapgos.2430.

[4] D. Bakhtiiarov, B. Chumachenko, O. Lavrynenko, V. Chupryn, V. Antonov, Distribute load among concurrent servers, in: CEUR Workshop Proceedings, volume 3826, CEUR-WS.org, 2024, pp. 260–266. URL: https://ceur-ws.org/Vol-3826/short15.pdf.

[5] O. Sushchenko, et al., Integration of MEMS inertial and magnetic field sensors for tracking power lines, in: International Conference on Perspective Technologies and Methods in MEMS Design (MEMSTECH), 2022, pp. 33–36. doi:10.1109/MEMSTECH55132.2022.10002907.

[6] S. Jawhar, C. E. Kimble, J. R. Miller, Z. Bitar, Enhancing cyber resilience with ai-powered cyber insurance risk assessment, in: 2024 IEEE 14th Annual Computing and Communication Workshop and Conference (CCWC), 2024, pp. 0435–0438. doi:10.1109/CCWC60891.2024.10427965.

[7] A. A. Sunna, T. Sultana, N. Kshetri, M. M. Uddin, Assesscica: Assessing and mitigating financial losses from cyber attacks with role of cyber insurance in post-pandemic era, in: 2025 13th International Symposium on Digital Forensics and Security (ISDFS), 2025, pp. 1–6. doi:10.1109/ISDFS65363.2025.11012092.

[8] D. Bakhtiiarov, B. Chumachenko, O. Lavrynenko, V. Antonov, Evaluating the uav's communication channels energy availability in the context of enemy electronic countermeasures, 2024 IEEE 7th International Conference on Actual Problems of Unmanned Aerial Vehicles Development, APUAVD 2024 - Proceedings (2024) 159–164. doi:10.1109/APUAVD64488.2024.10765900.

[9] N. Yehorov, M. Zaliskyi, B. Chumachenko, D. Bakhtiiarov, A method for deterministic signal detection on the background of noise based on the neural network, in: Proceedings of the 2024 IEEE 5th KhPI Week on Advanced Technology (KhPIWeek), IEEE, Kharkiv, Ukraine, 2024, pp. 1–6. doi:10.1109/KhPIWeek61434.2024.10878073.

[10] O. Sushchenko, et al., Airborne sensor for measuring components of terrestrial magnetic field, in: IEEE International Conference on Electronics and Nanotechnology (ELNANO), 2022, pp. 687–691. doi:10.1109/ELNANO54667.2022.9926760.

[11] R. Odarchenko, A. Pinchuk, O. Polihenko, A. Skurativskyi, A comparative analysis of cyber threat intelligence models, CEUR Workshop Proceedings 3925 (2025) 3–12. URL: https://ceur-ws.org/Vol-3925/paper01.pdf.

[12] R. Odarchenko, V. Pevnev, A. Pinchuk, O. Polihenko, Optimization of the integrated video surveillance system with elements of data analysis, CEUR Workshop Proceedings 3925 (2025) 47–63. URL: https://ceur-ws.org/Vol-3925/paper05.pdf.

[13] M. Abdollahi, R. Sabzalizadeh, S. Javadinia, S. Mashhadi, S. S. Mehrizi, A. Baniasadi, Automatic modulation classification for nlos 5g signals with deep learning approaches, in: Proceedings of the 2023 10th International Conference on Wireless Networks and Mobile Communications (WINCOM), IEEE, Istanbul, Turkiye, 2023, pp. 1–6. doi:10.1109/WINCOM59760.2023.10322928.

[14] G. Tonn, J. P. Kesan, L. Zhang, J. Czajkowski, Cyber risk and insurance for transportation infrastructure, Transport Policy 79 (2019) 103–114. URL: https://www.sciencedirect.com/science/article/pii/S0967070X18307248. doi:10.1016/j.tranpol.2019.04.019.

[15] S. J. Aljarrah, S. Cherbal, A. Mashaleh, J. A. Karaki, A. Gawanmeh, On the comparative analysis of trends in cybersecurity risk assessment, governance, and compliance frameworks, in: 2024 International Jordanian Cybersecurity Conference (IJCC), 2024, pp. 136–142. doi:10.1109/IJCC64742.2024.10847280.

[16] P. Sadhukhan, J. Bhaumik, Automatic modulation classification using convolutional neural network with batch normalization: A novel approach, in: Proceedings of the 2024 4th International Conference on Computer, Communication, Control & Information Technology (C3IT), IEEE, Hooghly, India, 2024, pp. 1–4. doi:10.1109/C3IT60531.2024.10829439.

[17] D. I. Putra, S. Ekariani, Enhancing the coexistence of 802.11 wlan and 5g networks using a multi-task learning with convolutional neural network model, in: Proceedings of the 2024 2nd International Symposium on Information Technology and Digital Innovation (ISITDI), IEEE, Bukittinggi, Indonesia, 2024, pp. 167–172. doi:10.1109/ISITDI62380.2024.10796737.

[18] K. S. Mayer, C. Müller, J. A. Soares, F. C. C. de Castro, D. S. Arantes, Deep phase-transmittance rbf neural network for beamforming with multiple users, IEEE Wireless Communications Letters 11 (2022) 1498–1502. doi:10.1109/LWC.2022.3177162.

[19] M. Zaliskyi, et al., Model building for diagnostic variables during aviation equipment maintenance, in: International Scientific and Technical Conference on Computer Sciences and Information Technologies (CSIT), 2022, pp. 160–164. doi:10.1109/CSIT56902.2022.10000556.

[20] B. Shamasundar, S. Venkatesh, G. D. Surabhi, A. K. R. Chavva, Ai-aided opportunistic quantization for channel aging mitigation and fronthaul overhead reduction in o-ran systems, in: Proceedings of the 2024 IEEE 100th Vehicular Technology Conference (VTC2024-Fall), IEEE, Washington, DC, USA, 2024, pp. 1–5. doi:10.1109/VTC2024-Fall63153.2024.10757837.

[21] O. Solomentsev, M. Zaliskyi, T. Herasymenko, O. Kozhokhina, Y. Petrova, Efficiency of operational data processing for radio electronic equipment, Aviation 23 (2020) 71–77. doi:10.3846/aviation.2019.11849.

[22] J. Pihlajasalo, et al., Deep learning ofdm receivers for improved power efficiency and coverage, IEEE Transactions on Wireless Communications 22 (2023) 5518–5535. doi:10.1109/TWC.2023.3235059.

[23] X. Chen, X. Wang, H. Zhao, Z. Fei, Deep learning-based joint modulation and coding scheme recognition for 5g new radio protocols, in: 2022 IEEE 22nd International Conference on Communication Technology (ICCT), 2022, pp. 1411–1416. doi:10.1109/ICCT56141.2022.10072789.

[24] M. Zaliskyi, Y. Petrova, M. Asanov, E. Bekirov, Statistical data processing during wind generators operation, International Journal of Electrical and Electronic Engineering and Telecommunications 8 (2019) 33–38. doi:10.18178/ijeetc.8.1.33-38.

[25] G. Dede, A. M. Petsa, S. Kavalaris, E. Serrelis, S. Evangelatos, I. Oikonomidis, T. Kamalakis, Cybersecurity as a contributor toward resilient internet of things (iot) infrastructure and sustainable economic growth, Information 15 (2024). doi:10.3390/info15120798.

[26] H. Li, Computer network connection enhancement optimization algorithm based on convolutional neural network, in: 2021 International Conference on Networking, Communications and Information Technology (NetCIT), 2021, pp. 281–284. doi:10.1109/NetCIT54147.2021.00063.

[27] J. P. Nzabahimana, Analysis of security and privacy challenges in internet of things, in: 2018 IEEE 9th International Conference on Dependable Systems, Services and Technologies (DESSERT),

2018, pp. 175–178. doi:10.1109/DESSERT.2018.8409122.

[28] O. Solomentsev, M. Zaliskyi, O. Kozhokhina, T. Herasymenko, Efficiency of data processing for UAV operation system, in: IEEE 4th International Conference on Actual Problems of Unmanned Aerial Vehicles Developments (APUAVD), 2017, pp. 27–31. doi:10.1109/APUAVD.2017.8308769.

[29] P. Ruijie, A. Sali, L. Li, M. Z. Mohyedin, S. Qahtan, Evaluation of personal radiation exposure from wireless signals in indoor and outdoor environments, IEEE Access 13 (2025) 106489–106510. doi:10.1109/ACCESS.2025.3579085.

[30] T. Song, C. Lim, A. Nirmalathas, Performance analysis of a 28 ghz wideband analog radio-over-fiber fronthaul with channel nonlinearity compensation, Journal of Lightwave Technology 42 (2024) 7588–7595. doi:10.1109/JLT.2024.3416046.

[31] O. Solomentsev, M. Zaliskyi, O. Zuiev, Estimation of quality parameters in the radio flight support operational system, Aviation 20 (2016) 123–128. doi:10.3846/16487788.2016.1227541.

[32] M. H. Rahman, M. Shahjalal, Y. M. Jang, Ensemble classifier based modulation recognition for beyond 5g massive mimo (mmimo) communication, in: 2021 International Conference on Artificial Intelligence in Information and Communication (ICAIIC), 2021, pp. 483–487. doi:10.1109/ICAIIC51459.2021.9415269.

[33] E. S. Hidalgo, J. Xavier Salvat Lozano, J. A. Ayala-Romero, A. Garcia-Saavedra, X. Li, X. Costa-Perez, Memorai: Energy-efficient last-level cache memory optimization for virtualized rans, in: 2024 IEEE International Conference on Machine Learning for Communication and Networking (ICMLCN), 2024, pp. 25–30. doi:10.1109/ICMLCN59089.2024.10624821.

[34] O. Lavrynenko, R. Odarchenko, G. Konakhovych, A. Taranenko, D. Bakhtiiarov, T. Dyka, Method of semantic coding of speech signals based on empirical wavelet transform, in: 2021 IEEE 4th International Conference on Advanced Information and Communication Technologies (AICT), 2021, pp. 18–22. doi:10.1109/AICT52120.2021.9628985.

[35] M. Khalid, S. Omatu, A neural network based control scheme with an adaptive neural model reference structure, in: [Proceedings] 1991 IEEE International Joint Conference on Neural Networks, 1991, pp. 2128–2133 vol.3. doi:10.1109/IJCNN.1991.170702.